AIAA JOURNAL
Vol. 37, No. 7, July 1999

Effects of Perpendicular Blade–Vortex Interaction, Part 2: Parameter Study

K. S. Wittmer* and W. J. Devenport†
Virginia Polytechnic Institute and State University, Blacksburg, Virginia 24061-0203
and
S. A. L. Glegg‡
Florida Atlantic University, Boca Raton, Florida 33431

Experiments have been performed to document the turbulent flow produced downstream of an airfoil encountering an intense streamwise vortex. In the second part of two-part paper, measurements revealing the effects of blade–vortex separation, blade angle of attack, and vortex strength are presented. The purpose is to provide the data needed to improve blade–vortex and blade–wake interaction noise prediction schemes to account for these effects. A total of 48 flows were studied by measuring three-component velocity and turbulence stress profiles and spectra through the vortex core downstream of the interaction. Most measurements were made 15 chordlengths downstream of the blade trailing edge. These measurements show, consistent with an inviscid model, that the effects of the interaction are only weakly dependent on blade angle of attack and vortex strength and on whether the vortex passes to the suction or pressure side of the blade. The interaction has little influence on the properties of the vortex core for separations greater than about 0.3 chords. For smaller separations, the interaction substantially weakens the vortex core and increases its size, these effects increasing as the separation is reduced. For separations near zero, the vortex is all but destroyed, the peak tangential velocity of the vortex core being reduced by more than an order of magnitude.

Introduction and Apparatus

PERPENDICULAR blade–vortex interactions are a common occurrence in helicopter rotors during level flight and mild climb conditions.[1] The nature of these interactions is a function of (among other things) the blade–vortex separation, the vortex strength, and the blade angle of attack. The influence these interactions have on the noise generated by subsequent perpendicular or parallel encounters is also a function of the rate of decay of the disturbed vortex over the intervening period. The objective of this paper is to present measurements that reveal the effects of a perpendicular blade on a trailing vortex flow as functions of these variables. Such data are an essential part of the development of empirical methods to account for the influence of prior perpendicular blade–vortex interactions (BVIs) in BVI and blade–wake interaction noise prediction schemes.

Measurements were made using the same wind tunnel and configuration described in Part 1 of this paper.[2] The wind tunnel and configuration consisted of a rectangular NACA 0012 blade used to generate the tip vortex and similar blade, spanning the complete test section, to interact with it some 14 chordlengths c downstream (see Fig. 1 of Ref. 2). Measurements downstream of the interaction blade were made using hot-wire anemometry (the same three-component four-sensor system described in Ref. 2) for a range of blade–vortex separations, initial vortex strengths (controlled by the angle of attack of the vortex generator, α_g), and blade angles of attack α_b. The blade–vortex separation Δ was adjusted by varying the z position of the interaction blade. $\Delta = 0$ corresponds to the z position of the blade at which the streamline marking the vortex center (visualized with helium-filled soap bubbles) was seen to stagnate on the blade leading edge. Note that this position varies with both α_g and α_b and, thus, had to be re-established for each angle-of-attack combination. All measurements were made at a chord Reynolds number of 5.3×10^5. Boundary-layer measurements at the blade trailing edges, uncertainty estimates, and a nomenclature are given in Ref. 2.

Received 4 December 1997; revision received 16 January 1999; accepted for publication 23 January 1999.

*Research Associate, Department of Aerospace and Ocean Engineering; currently Handling Qualities Engineer, Sikorsky Aircraft Corporation, Stratford, CT 06615.
†Associate Professor, Department of Aerospace and Ocean Engineering. Senior Member AIAA.
‡Professor, Department of Ocean Engineering. Senior member AIAA.

Results and Discussion

Three-component velocity and turbulence stress measurements were made in z-wise profiles through the vortex center (see Fig. 1 of Ref. 2 for definition of the coordinate system used). The core center was determined before measuring each profile by traversing the probe over the vortex cross section to locate the point of zero mean crossflow velocity. Velocity spectra were also measured at the core center as an indicator of the turbulence structure there. Measurements were made in a total of 48 different flows produced using different combinations of Δ, α_g, and α_b. The full test matrix is listed in Table 1. The vast bulk of the measurements were made at $x/c = 30$, 15 chordlengths downstream of the trailing edge of the interaction blade.

Effects of Blade Vortex Separation

Velocity profiles were measured through the vortex at $x/c = 30$ with the generator and interaction blades both at 5-deg angle of attack for some 14 different blade–vortex separations Δ from $-0.5c$ to $0.5c$. Note that this baseline variation, as we shall refer to it, includes the flow described in Part 1 (Ref. 2) with $\Delta = -0.125c$.

Mean axial and tangential velocity profiles are plotted in Fig. 1 against $z - z_0$ where z_0 identifies the vortex core center. This and subsequent figures for the baseline variation include only data for pressure-side encounters ($\Delta \leq 0$); the measurements for suction-side encounters of the same absolute blade–vortex separation are only slightly different.

For blade–vortex separation magnitudes larger than about $0.3c$, the mean-velocity field of the vortex core is almost unaffected by the interaction, and the tangential and axial velocity profiles are almost identical to those measured by Devenport et al.[3] with the interaction blade removed. These profiles reveal an intense vortex core of peak tangential velocity $V_{\theta_1} = 0.27U_\infty$, core radius $r_1 = 0.04c$, and centerline axial velocity deficit $U_d = 0.13U_\infty$. The implied core circulation $\Gamma = 2\pi r_1 V_{\theta_1} = 0.068cU_\infty$ is some 28% of the total bound circulation on the vortex generator Γ_0. As the separation magnitude is reduced below $0.3c$, the effects of the interaction rapidly become significant. Both the tangential and axial velocity profiles weaken

Table 1 Measurement locations and conditions for study of interaction parameters

x/c	α_g, deg	α_b, deg	Δ/c
15.16	5	5	±0.125
15.95	5	5	±0.125
17.5	5	5	±0.125
20	5	5	±0.125
22.5	5	5	±0.125
25	5	5	±0.125
30	5	5	±0.125
30	5	5	±0.5
30	5	5	±0.375
30	5	5	±0.25
30	5	5	±0.125
30	5	5	±0.0938
30	5	5	±0.0625
30	5	5	±0.0312
30	5	5	0
30	5	0	0.375
30	5	0	0.25
30	5	0	0.125
30	5	0	0.0938
30	5	0	0.0625
30	5	0	0.0312
30	5	0	0
30	10	5	0.5
30	10	5	0.375
30	10	5	0.25
30	10	5	0.125
30	10	5	0.0938
30	10	5	0.0625
30	10	5	0.0312
30	10	5	0
30	5	2.5	−0.125
30	5	5	−0.125
30	5	7.5	−0.125
30	2.5	2.5	−0.125
30	3.75	3.75	−0.125
30	5	5	−0.125
30	6.25	6.25	−0.125
30	7.5	7.5	−0.125
30	10	10	−0.125

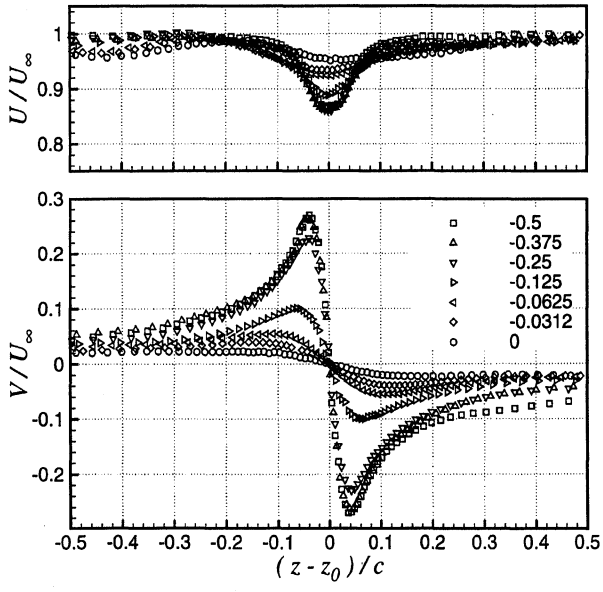

Fig. 1 Mean axial and tangential velocity profiles for pressure-side encounters ($x/c = 30$, $\alpha_g = \alpha_b = 5$ deg); numbers in legend are Δ/c values.

substantially, the peak tangential velocity falling by an order of magnitude as the separation is reduced to zero. The core radius also increases, but by a lesser amount, and as a result the core circulation at $\Delta = 0$ is only $0.1\Gamma_0$. This drop in core circulation is a direct result of the ingestion into the core of the negative vorticity shed by the blade under the influence of the vortex.

Considering the complex turbulence structure of this flow, e.g., Fig. 2, Ref. 2, the mean velocity profiles remain remarkably symmetric at smaller blade–vortex separations. Some flow asymmetry can be seen in the profiles of the axial normal turbulent stress $\overline{u^2}$ (Fig. 2). Turbulence levels are consistently larger on the side of the vortex, where the blade wake is initially located: the negative z side for $\Delta > 0$ and the positive z side for $\Delta < 0$. For blade–vortex separations of $\pm 0.5c$, turbulence levels are elevated only in the core and blade wake, which remain essentially separate. (Note that the peak in turbulence levels corresponding to the blade wake lies outside the range of Fig. 2 for $\Delta/c = -0.5$.) U-component velocity spectra G_{uu} measured at the core center (Fig. 3) show very low levels at higher frequencies ($fc/U_\infty > 20$), an indication that the cores are probably laminar.[3] Therefore, it is likely that the $\overline{u^2}$ levels seen in the core at these separations are primarily a product of vortex wandering. Note that the influence of wandering on turbulence levels measured in the core at smaller separations would have been less because of the larger core size and smaller axial velocity deficit that the interaction produces.

As the magnitude of the blade–vortex separation is reduced below $0.375c$, the turbulence produced by the wake and vortex core merge into a single wide region of elevated turbulence levels, at least $0.7c$ across. The spanwise extent of the turbulent region encountered by a subsequent blade is an important parameter in the prediction of the noise produced by the interaction using a method such as Glegg's.[4] With the interaction between the core and the wake becoming significant, the core center spectra show an order

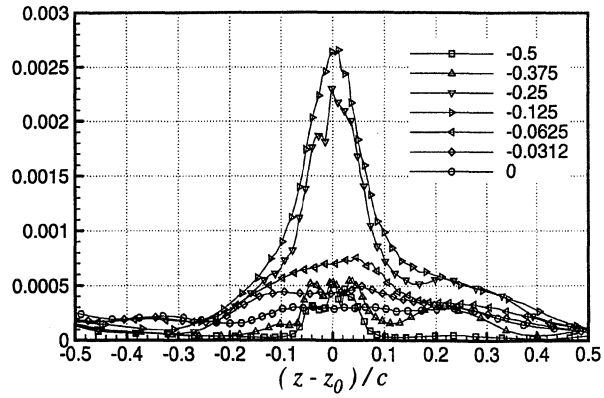

Fig. 2 Profiles of $\overline{u^2}/U_\infty^2$ for pressure-side encounters ($x/c = 30$, $\alpha_g = \alpha_b = 5$ deg); numbers in legend are Δ/c values.

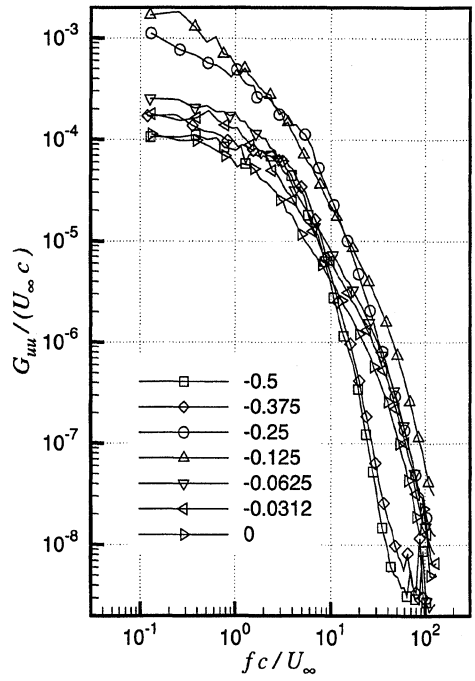

Fig. 3 Core center velocity autospectra following pressure side encounters ($x/c = 30$, $\alpha_g = \alpha_b = 5$ deg); numbers in legend are Δ/c values.

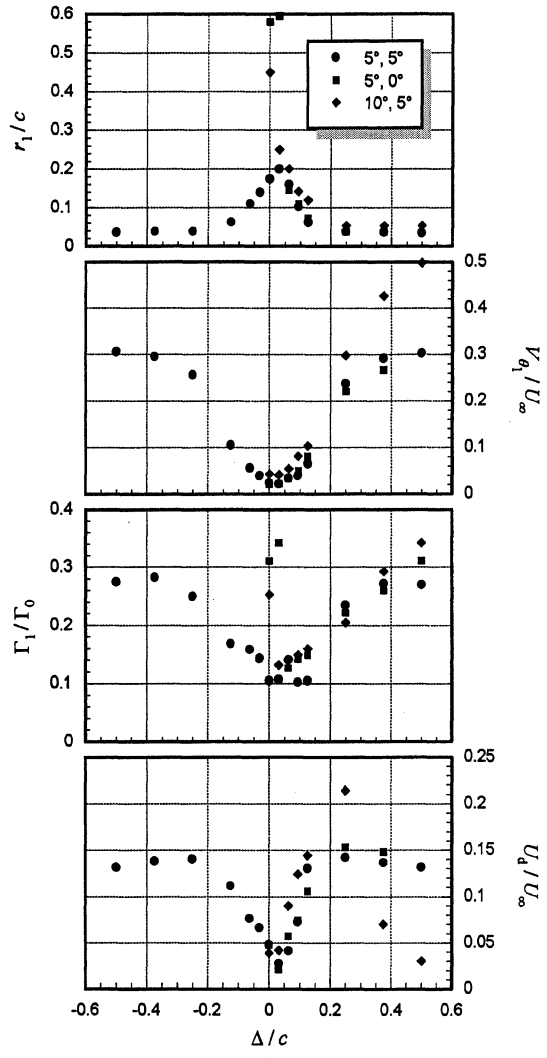

Fig. 4 Core parameters at $x/c = 30$ as a function of blade–vortex separation for different blade angles of attack; numbers in legend are α_g and α_b values.

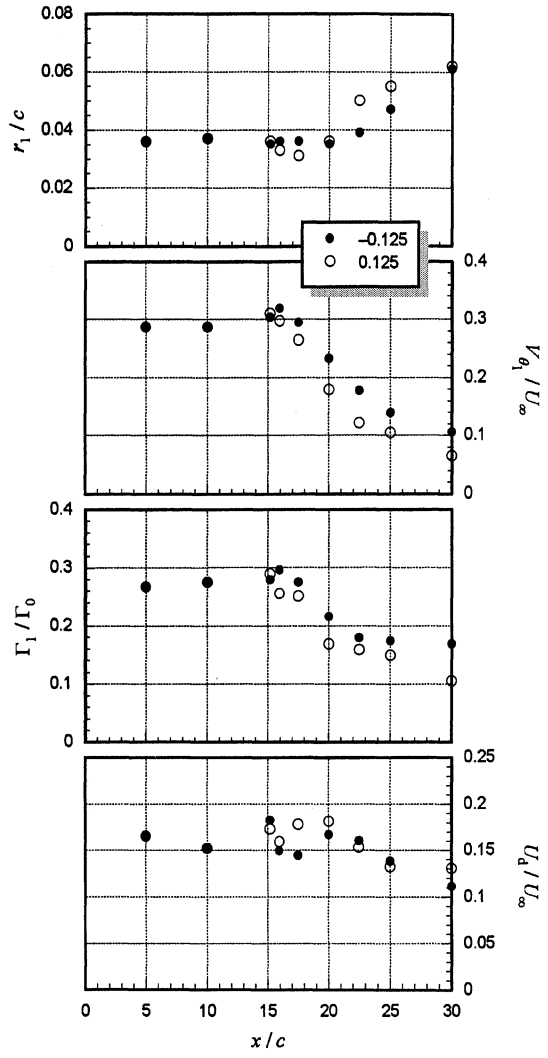

Fig. 5 Core parameters as a function of downstream distance for pressure- and suction-side encounters of $|\Delta/c| = 0.125$ ($\alpha_g = \alpha_b =$ 5 deg); numbers in legend are Δ/c values.

of magnitude increase in high-frequency ($fc/U_\infty > 20$) spectral levels, which may indicate the presence of turbulence in the core. Interestingly, the highest turbulence and spectral levels are found at a separation magnitude of around $0.2c$. For larger separations, turbulence levels produced by the unstable interaction between the core and blade wake may still be growing. For smaller separations they may already be dying out.

The variations visible in mean velocity profiles are summarized in Fig. 4, where core parameters (r_1, V_{θ_1}, U_d, and Γ_1) are plotted as functions of Δ/c. The parameters have been adjusted to account for the vortex wandering using the method of Devenport et al.[3] Figure 4 shows that the BVI influences the peak tangential velocity and core circulation over a broader range of blade–vortex separations than it does the core size or axial velocity deficit. Interestingly, they also show that BVI has the largest influence on the core parameters not at zero blade–vortex separation but at a slightly positive Δ/c of about 0.03. This, we suspect, is the result in a change in the nature of the interaction for very small blade–vortex separations. Rife and Devenport[5] performed extensive helium bubble flow visualizations to reveal the fate of a vortex core passing a part-span blade as a function of blade–vortex separation. They found, consistent with the results of Part 1 (Ref. 2), that for blade–vortex separations outside the range of $-0.0625 \leq \Delta \leq 0.0312c$, the vortex passes the blade essentially unaltered. However, for smaller separations, they found a range of complex phenomena, including spiral and bubble bursting of the vortex and splitting of the vortex at the blade leading edge, that were not symmetric with respect to zero separation. These effects appeared to be produced by the direct influence of the intense pressure field immediately surrounding the blade on the vortex core.

Except for these effects at small separations, the variations in core parameters are fairly symmetric about $\Delta = 0$, indicating that the ultimate form of the vortex is not greatly influenced by whether it passes to the suction or pressure side of the blade. Such a symmetry might be expected given the analysis presented in Part 1 (Ref. 2), which showed that, at least to an inviscid approximation, the negative vorticity shed from the blade trailing edge that causes the disruption to the vortex core depends only on the magnitude of the blade–vortex separation.

This symmetry in flow behavior is examined further in Fig. 5, where we compare the streamwise development of vortex core parameters (inferred from z-wise mean velocity profiles) for blade–vortex separations of $0.125c$ and $-0.125c$. The interaction of the negative vorticity and turbulence in the blade wake with the vortex core produces essentially the same effects in both flows, a rapid increase in core radius and weakening of its strength and axial velocity deficit, at approximately the same streamwise locations. For the suction-side passage ($\Delta/c = 0.125$), the drop in the core circulation and peak tangential velocity is slightly greater and occurs slightly farther upstream than for the pressure-side passage. This difference probably results because for suction-side passages the vortex core is initially closer to the blade wake than for pressure-side passages. This is shown in Fig. 6, where we plot z-wise mean axial velocity profiles measured through the core center at $x/c = 15.16$ ($0.16c$ downstream of the blade trailing edge) for $\Delta/c = -0.125$ and 0.125. Both profiles show the same regions of axial velocity deficit associated with the vortex core and the blade wake, but for the suction-side passage ($\Delta/c = 0.125$), the two are about $0.04c$ closer.

Table 2 Core parameters from investigation of interaction blade angle-of-attack effects

x/c	α_g, deg	α_b, deg	Δ/c	r_1/c	V_{θ_1}/U_∞	Γ_1/Γ_0	U_d/U_∞
30	5	2.5	−0.125	0.052	0.123	0.167	0.116
30	5	5	−0.125	0.061	0.105	0.168	0.111
30	5	7.5	−0.125	0.068	0.093	0.164	0.098

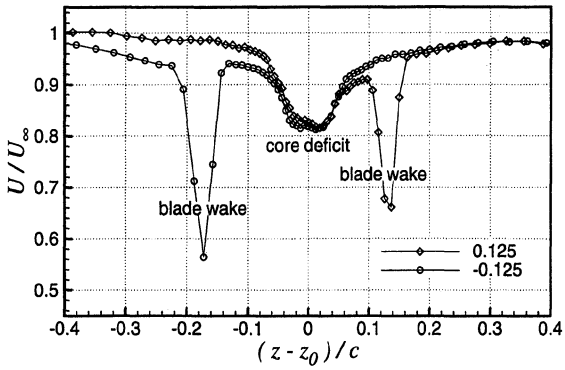

Fig. 6 Mean axial velocity profiles measured at $x/c = 15.16$ ($\alpha_g = \alpha_b = 5$ deg); numbers in legend are Δ/c values.

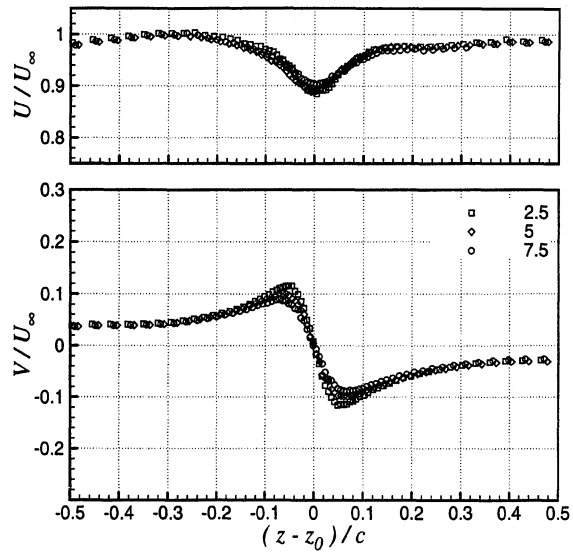

Fig. 7 Mean axial and tangential velocity profiles for various blade angles of attack ($x/c = 30$, $\alpha_g = 5$ deg, $\Delta/c = -0.125$); numbers in legend are α_b values.

The comparison of the streamwise variations of Fig. 5, with those due to blade–vortex separation in Fig. 4, suggests some interplay between these two factors. Specifically, for small blade–vortex separations, the interaction between the vortex and blade wake is likely to begin almost immediately downstream of the blade trailing edge, and thus at $x/c = 30$ we see in the results the long-term consequences of the interaction. For larger separations, the interaction is delayed until there is sufficient contact between the two flow regions, e.g., until about $x/c = 20$ in Fig. 5, and we see its more recent effects in the results at $x/c = 30$.

Effects of Blade Angle of Attack

Two sequences of velocity profile measurements were made at $x/c = 30$ with the vortex generator at 5-deg angle of attack to reveal the effects of blade angle of attack on the ultimate form of the vortex. First, the measurements of the baseline variation were repeated, but with the blade angle of attack reduced to 0 deg. Second, measurements were made for a fixed blade–vortex separation of $\Delta/c = -0.125$ for blade angles of attack of 0, 2.5, 5, and 7.5 deg.

The first set of measurements resulted in the velocity profiles summarized in terms of core parameters and compared to the baseline variation in Fig. 4. All encounters were considered to be suction side ($\Delta \geq 0$) because the vortex passed on what would have been the suction side of the blade if it were at a positive angle of attack as in the baseline variation. These data show the effects of the interaction to be largely independent of the blade angle of attack. This might be expected because the inviscid analysis of Part 1 (Ref. 2) showed that the vortex sheet shed from the blade is independent of its angle of attack; changes to the core have been shown to occur primarily due to its interaction with the negative part of that sheet. Turbulence profiles and velocity autospectra (not shown) are similar to the baseline variation. High-frequency velocity fluctuations measured in the core center indicate that it is turbulent for separations of $0.25c$ and less. The only significant effects of blade angle of attack are seen in the core radius for blade–vortex separations less than the initial core size of $0.037c$. For such close separations, the vortex core might be split or otherwise locally modified by the blade,[5] complicating the flowfield greatly, and it is unlikely that such splitting effects would be independent of the interaction blade angle of attack.

The results of the second set of measurements are shown in terms of the z-wise mean velocity profiles (Fig. 7) and the corresponding core parameters listed in Table 2. Here we do see a small effect of blade angle of attack. A blade angle of attack of 2.5 deg produces a core radius of $0.052c$, peak tangential velocity of $0.123U_\infty$, and centerline axial velocity deficit of $0.116U_\infty$ at $x/c = 30$. For $\alpha_g = 7.5$ deg, these values are $0.068c$, $0.093U_\infty$, and $0.098U_\infty$, respectively; the values for $\alpha_g = 5$ deg fall in between. Interestingly, these numbers imply a variation in core circulation of less than 3%. These relatively mild effects of blade angle of attack could have a number of causes such as: differences in the separation pattern on the blade under the vortex, differences in the strength of the blade wake with angle of attack, and compression of the vortex by the pressure field surrounding the blade. At first sight it does not appear that compression could account for all of the effects seen. One expects pure compression to produce equal percentage reductions in the angular velocity at the core center (roughly proportional to V_{θ_1}/r_1) and the axial velocity there, which are not seen here. However, this inviscid argument ignores the subsequent turbulent decay.

Vortex Strength Effects

To examine the effects of initial vortex strength on the variation of core parameters with blade–vortex separation, measurements were made with the vortex generator at an angle of attack of 10 deg. All other factors were the same as the baseline variation. The core parameters are plotted as functions of blade–vortex separation in Fig. 4 along with values for the baseline variation. Initially, the effects of the interaction appear heavily dependent on the generator angle of attack, although in both cases, as the magnitude of the blade–vortex separation is decreased, a decrease in peak tangential velocity occurs before the core radius is seen to increase. If these parameters are normalized on their undisturbed values measured at $x/c = 10$ ($r_1|_{10}$ and $V_{\theta_1}|_{10}$), then the effects of the generator angle of attack appear much weaker, as shown in Fig. 8. Because the strength of the vorticity shed by the blade would be proportional to the vortex strength, the nature of the interaction, therefore, appears to be more dependent on the spatial arrangement of the vorticity field than it is on the absolute strengths of the vorticity regions involved.

Although the measurements presented thus far imply that the mean flow effects of the interaction are nearly independent of the interaction blade angle of attack and only weakly dependent on the vortex strength for separations where the vortex has not burst or split, these generalizations should be carefully applied. To stretch the application of those findings, measurements were also made at $x/c = 30$ with a fixed blade–vortex separation of $-0.125c$ for a range of vortex strengths (controlled by α_g) and blade angles of attack α_b, where $\alpha_g = \alpha_b$. Angles studied were from 2.5 to 10 deg. Based on our findings, we would expect little change in the core parameters normalized on their initial values. However, the core parameters listed in Table 3 do show some angle-of-attack effects. For $\alpha_g = \alpha_b = 2.5$ and 3.25 deg, there is no loss in core circulation, whereas there are 40–50% losses for the other cases.

Table 3 Core parameters from investigation of angle-of-attack effects

x/c	$\alpha_g = \alpha_b$, deg	Δ/c	r_1/c	V_{θ_1}/U_∞	Γ_1/Γ_0	U_d/U_∞	$r_1/r_1\|_{10}$	$V_{\theta_1}/V_{\theta_1}\|_{10}$	$\Gamma_1/\Gamma_1\|_{10}$
30	2.5	−0.125	0.058	0.056	0.170	0.065	3.05	0.34	1.03
30	3.75	−0.125	0.055	0.093	0.178	0.092	2.62	0.40	1.05
30	5	−0.125	0.061	0.105	0.168	0.111	1.65	0.37	0.61
30	6.25	−0.125	0.072	0.110	0.166	0.114	1.76	0.31	0.55
30	7.5	−0.125	0.104	0.093	0.168	0.111	2.31	0.22	0.51
30	10	−0.125	0.300	0.054	0.212	0.055	5.66	0.11	0.61

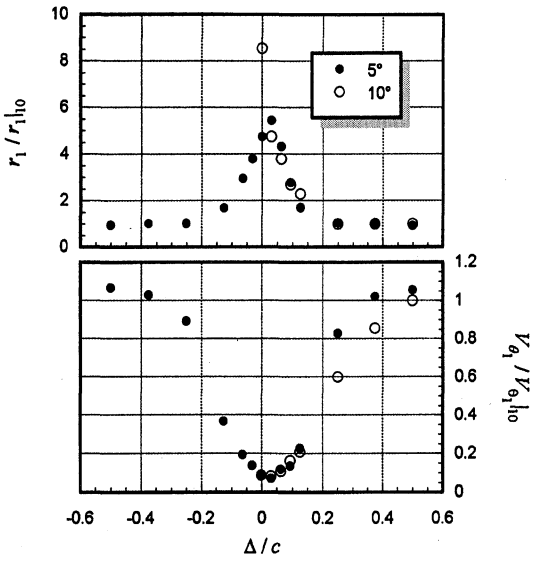

Fig. 8 Core parameters as a function of blade–vortex separation for two different generator angles of attack normalized on undisturbed values ($x/c = 30$, $\alpha_b = 5$ deg); numbers in legend are α_g values.

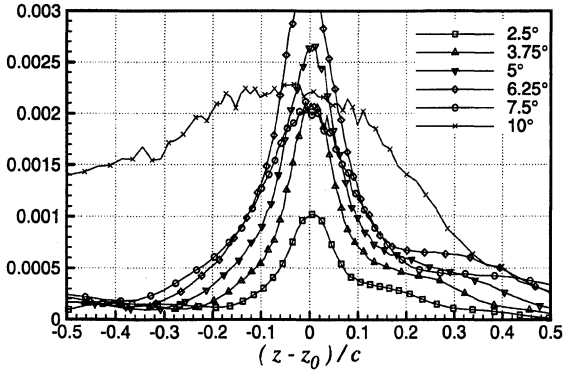

Fig. 9 Profiles of $\overline{u^2}/U_\infty^2$ for investigation of angle-of-attack effects ($x/c = 30$, $\Delta/c = -0.125$); numbers in legend are $\alpha_g = \alpha_b$ values.

Turbulence profiles (Fig. 9) show an intensification and broadening of the turbulent region as the angles of attack increase. Velocity autospectra measured in the core centers (not shown) indicate turbulence in the vortex core in every case. We suspect that the larger changes in normalized core parameters produced by the interaction for 10 deg are produced by bursting of the core by the more intense pressure field surrounding the blade, such as observed by Rife and Devenport.[5]

Conclusions

Experiments have been performed to document the effects of a perpendicular interaction on a tip vortex as a function of blade–vortex separation, blade angle of attack, and vortex strength. A total of 48 flows were studied by measuring three-component velocity and turbulence stress profiles and spectra through the vortex core downstream of the interaction. Most measurements were made 15 chordlengths downstream of the blade trailing edge. On the basis of analysis of these measurements, we draw the following conclusions:

1) For blade–vortex separation magnitudes greater than about $0.3c$, the interaction has little influence on the mean velocity field of the vortex core.

2) For blade–vortex separations less than $0.3c$, the interaction substantially weakens the vortex core and increases its size, these effects increasing as the separation is reduced.

3) For a blade–vortex separation of zero, the interaction causes more than an order of magnitude reduction in the peak tangential velocity and a large increase in the core radius. The core circulation is also reduced by the injestion of the negative vorticity shed from the blade.

4) Except for very small separations ($<0.1c$), where the vortex may be burst or split by the blade, the effects of the interaction on the vortex are not greatly influenced by whether it passes to the suction or pressure side of the blade.

5) Except for small blade–vortex separations, the effects of the interaction on the vortex are only weak functions of the blade angle of attack and the vortex strength.

6) For separation magnitudes less than 0.3, the vortex core becomes turbulent following the interaction. The core and the blade wake combine to produce a single turbulent region typically $0.7c$ across. Turbulence levels generated by the interaction at $x/c = 30$ are largest for a separation magnitude of about $0.2c$.

Conclusions 1 and 5 are consistent with the inviscid model of the interaction presented in Part 1 (Ref. 2).[§]

Acknowledgments

The authors would like to thank NASA Langley Research Center, in particular Thomas F. Brooks and Casey L. Burley, for their work under Grant NAG-1-1539. The assistance of Gordon Follin and Mark Engel in taking many of the measurements presented is also gratefully acknowledged.

References

[1]Brooks, T. F., Marcolini, M. A., and Pope, D. S., "Main Rotor Broadband Noise Study in the DNW," *Journal of the American Helicopter Society*, Vol. 34, No. 2, 1989, pp. 3–12.

[2]Wittmer, K. S., and Devenport, W. J., "Effects of Perpendicular Blade–Vortex Interaction, Part 1: Turbulence Structure and Development," *AIAA Journal*, Vol. 37, No. 7, 1999, pp. 805–812.

[3]Devenport, W. J., Rife, M. C., Liapis, S. I., and Follin, G. J., "The Structure and Development of a Wing-Tip Vortex," *Journal of Fluid Mechanics*, Vol. 312, Jan. 1996, pp. 67–106.

[4]Glegg, S. A. L., "The Prediction of Blade–Wake Interaction Noise Based on a Turbulent Vortex Model," *AIAA Journal*, Vol. 29, No. 10, 1991, pp. 1545–1551.

[5]Rife, M. C., and Devenport, W. J., "Flow Visualizations of Perpendicular Blade Vortex Interactions," Dept. of Aerospace and Ocean Engineering, Virginia Polytechnic Inst. and State Univ., Rept. VPI-AOE-197, Blacksburg, VA, 1993.

P. R. Bandyopadhyay
Associate Editor

[§]The data discussed in this paper are available over the World Wide Web from http://www.aoe.vt.edu/flowdata/flowdata.html.